Progress In Electromagnetics Research M, Vol. 62, 41–50, 2017

Analysis and Validation of Super-Resolution Micro-Deformation Monitoring Radar

Zelong Shao[1, 2], Xiangkun Zhang[1, 2, *], and Yingsong Li[1, 3]

Abstract—A light micro-deformation monitoring radar based on frequency modulation continuous wave (FMCW) technique is proposed and designed for scenes which are sensitive to micro deformation such as slopes, dams, and high buildings. The miniradar is well suited to measure micro-deformation of buildings or mountains. Meanwhile, interferometric method was used by the radar to obtain high range resolution of the micro-deformation monitoring radar. The radar acquires micro deformation of the target by inversion of phase difference between the transmitted and received waves. To get an accurate micro-deformation measure result, the radar was carefully designed in signal mode and hardware structure. Various experiments are used in the article to verify the radar's deformation measure ability. The experiments prove that the radar can measure micro deformation accurately and timely. For example, railway bridges' vibration can be monitored by the radar in real time. In addition, it can be used in structures monitoring, disaster alarming and other regions.

1. INTRODUCTION

Deformation monitoring is a hot topic because it is of great importance in regions such as bridge monitoring, buildings maintenance and disaster alarming. A great number of deformation measure methods have been studied and used by using equipment such as global positioning system (GPS), total station and digital level [1]. However, most of them have disadvantages like high cost, complex data processing procedure [2]. Meanwhile, these instruments cannot measure the target's deformation in raining and fog environments. In addition, some of them should be in direct contact with the target. However, the requirement is difficult to satisfy in a harsh environment. Therefore, the radar proposed in the paper solves the problem by a remote sensing method and has a bright application prospect in the deformation monitoring field.

Radar is a system which uses echoes reflected by the target to calculate the target's parameters such as distance and velocity. For a long time, radars have been widely used in military for target detection, missile guidance and electronic countermeasures. However, most of them are large in size and heavy in weight. If we want to make the radar suitable for deformation monitoring, small micro-deformation monitoring radar is required in practical. The radar proposed in the paper is suitable for micro-deformation monitoring because of its weight and volume. In comparison with previous micro-deformation measure devices, frequency modulation continuous wave (FMCW) signals are used in the radar to make the system light [3]. In addition, the radar is an all-weather measure device, which is useful in remote sensing. In the last decades, radars using interferometric technique are studied and used in digital city, topographic mapping and disaster alarming [4]. Its non-contact characteristic insures

Received 26 July 2017, Accepted 28 October 2017, Scheduled 7 November 2017

* Corresponding author: Xiangkun Zhang (zhangxiangkun@mirslab.cn).

[1] Key Lab of Microwave Remote Sensing, National Space Science Centre, Beijing 100190, China. [2] School of Electronic, Electrical and Communication Engineering, University of Chinese Academy of Sciences, Beijing 100049, China. [3] College of Information and Communications Engineering, Harbin Engineering University, Harbin 150001, China.

that the radar acquires the target's deformation within the safe distance [5]. Thus, the radar is useful in a harsh environment such as abrupt slopes, snow-capped mountains and majestic icebergs.

Based on previous studies, FMCW radar was designed for micro-deformation measure field. Compared with radars which are based on vector network analyzer (VNA), the FMCW radar has advantages such as small size, light weight and low cost [6]. Various experiments are used to verify the viability and effectiveness of the radar. The experiments prove that the radar can measure vibrations accurately and timely. Thus, the radar is useful in micro-deformation monitoring.

The rest of this paper is organized as follows. Section 2 briefly reviews the micro-deformation measure principle of the radar and introduces the system structure of the radar. In Section 3, the radar's structure and its implementation are presented in detail. In Section 4, experiments are used to verify the effectiveness and accuracy of the radar. In Section 5, the radar is used to monitor a railway bridge's vibration. In Section 6, a short summary of this paper is given.

2. BASIC THEORY AND SYSTEM DESIGN

2.1. Measurement Theory

Herein, the principle of FMCW radar is described by means of the differential interferometric methods. As we know, the range resolution Δr of normal radar is determined by frequency bandwidth B of the transmitted signal [7, 8], which is given by the following equation.

$$\Delta r = \frac{c}{2B}, \tag{1}$$

where c represents the speed of light in vacuum. If we do not use interferometric technique, the range resolution of the radar will be 0.3 m when the bandwidth is 500 MHz. When the interferometric technique is used, the range resolution can be improved. The range resolution of the radar is influenced by the phase difference of echoes reflected by the target at different times. The relationship between the target's deformation and the phase difference can be described using the following equation [9, 10].

$$\Delta\phi = \frac{4\pi}{\lambda}\Delta r \tag{2}$$

When the radar is used to monitor a dam or a bridge, the deformation's precision is related with the precision of the phase measured by the radar. To acquire an accurate phase difference caused by the target's deformation, methods consist of phase unwrapping and atmospheric phase screen correction are used in the data processing procedure [11]. As the phase difference is smaller than 360° at one cycle, the range of the micro deformation is 4.16 mm at each cycle, when the frequency of the transmitted wave is 36.05 GHz. To broaden the measured range of the micro deformation, phase unwrapping is used in signal processing procedure. And, the measured distance between the target and the radar may be influenced by the atmosphere because the electromagnetic wave may be refracted in the transformation process. Thus, the atmospheric phase screen correction methods should be used in the signal processing procedure too.

2.2. System Description

The radar consists of transmitter and receiver modules. For transmitter module, direct digital synthesizer (DDS) generates signal which is supplied to amplifier (AMP), band pass filter (BPF), mixer, radio frequency filter (RF), coupler and isolator step by step. Then, the modulated signal is transmitted to the air via antennas. The transmitted signal reaches the target and is reflected by the target. Then, the receiver obtains the reflected signal. At the receiver side, the echo is obtained by the receive antenna. Then, the received signal is supplied to low noise amplifier (LNA), RF, mixer, BPF, auto gain control module (AGC), intermediate frequency amplifier (IF AMP), radio frequency flower (RFF) and analogy digital converter (ADC) step by step. Finally, the received signal is handled by the controller. The diagram of the proposed radar is shown in Fig. 1.

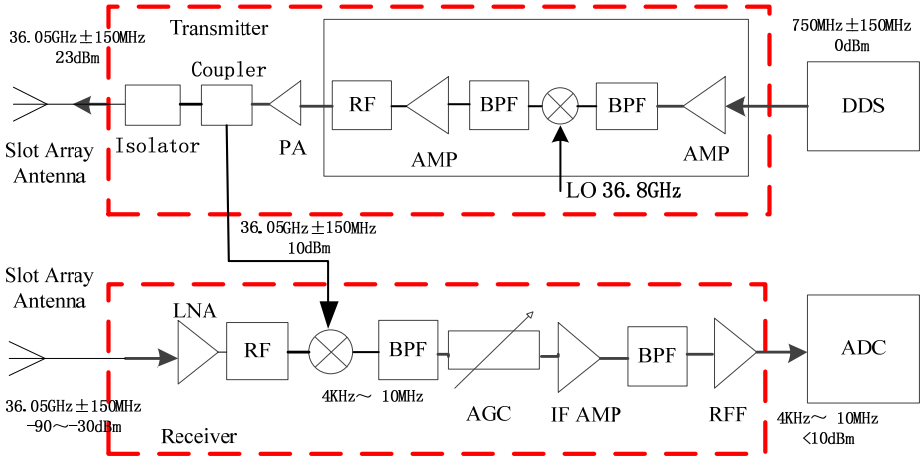

Figure 1. Block diagram of the radar.

3. HARDWARE IMPLEMENTATION

The microradar uses signals in Ka band whose center frequency is 36.05 GHz, and bandwidth is 300 MHz. Meanwhile, the deformation range of the target measured by the radar is obtained by Eq. (2). The phase accuracy measured by the radar is related with the system's signal noise ratio (SNR) [12]. The relationship between them can be described by Eq. (3). When the SNR of the radar system is greater than 19 dB, the precision of the measured phase difference less than 4.5°, and the radar measurement resolution can be 60 µm.

$$\Delta\phi^2 = 1/(2 \cdot \mathrm{SNR}) \tag{3}$$

In addition, hardware implement is very important in the design process of the radar. Firstly, two waveguide slot arrays at millimetre wave band are used for transmitting and receiving, respectively. Isolation between the transmitting and receiving antennas is set to 60 dB to insure the radar transmitting and receiving signals with a very low degree of coupling. Each antenna array has a beamwidth of $4° \times 10°$. Thus, the antennas used for transmitting or receiving can provide good directivity and high gain. The radiation pattern of the antenna array is shown in Fig. 2. It is obvious that the difference between the main beam and the first side-lobe is larger than 23 dB, and the main beam is narrower than the theoretical requirements proposed above. Thus, the antenna array can provide good side-lobe suppression ability.

Secondly, the origin chirp signal is generated by using a DDS module, which is shown in Fig. 3. It is realized by a DDS chip, a PLL block and others. The signal generation procedure is simple and flexible for the application of advanced microchips such as AD9914 and ADF4107. In the system, the chip AD9914 is used to generate frequency modulated chirp signal from low frequency to high frequency. To get higher linear sweep frequency signal, an FPGA controller is used to control the DDS chip [13]. Signal generated by AD9954 should pass a low-pass filter (LPF1) to eliminate the noise whose frequency is the multiple of the DDS chip's sampling clock. Because the sampling frequency of the AD9954 is only 400 MHz, output signal from the LPF1 should pass through phase-locked-loop module (PLL) to obtain the ideal chirp signal (750 MHz ± 150 MHz) which can be provided to the transmitter. The PLL is made up of Phase detector (PD), low-pass filter (LPF2), voltage Controlled Oscillator (VCO) and frequency divider (DIV).

Thirdly, the signal generated by the DDS module is passed to a band-pass filter and a mixer to get high frequency signal which is near the carrier frequency signal. After that, the signal is sent to the power amplifier to insure that the signal is strong enough after being transmitted into free space. Meanwhile, an LNA is used at the receiver side to get the weak echo reflected by the target in the complex environments. At the receiver side, the weak received echo signal passes though the mixer to remove the carrier wave and becomes intermediate frequency signal whose frequency is between 4 kHz

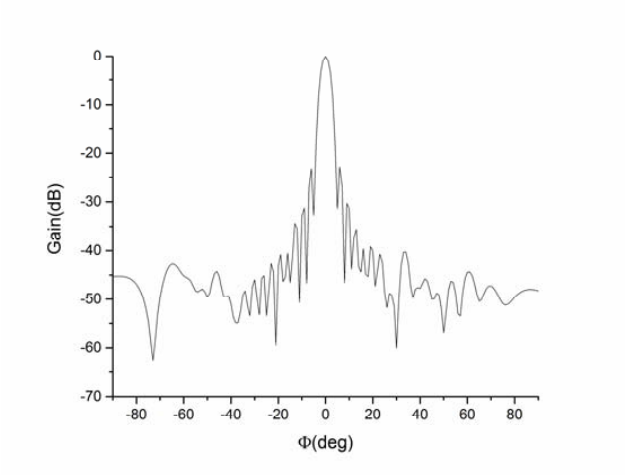

Figure 2. Radiation pattern of the antenna array.

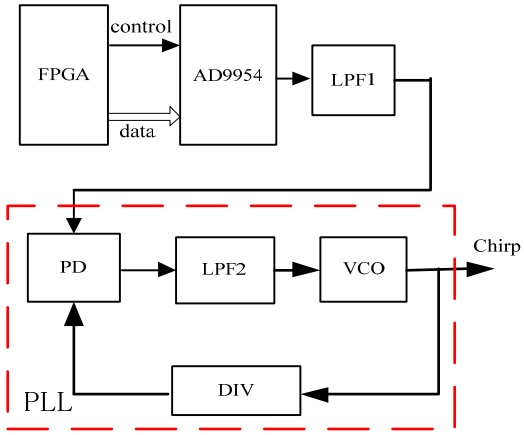

Figure 3. Block diagram of the DDS.

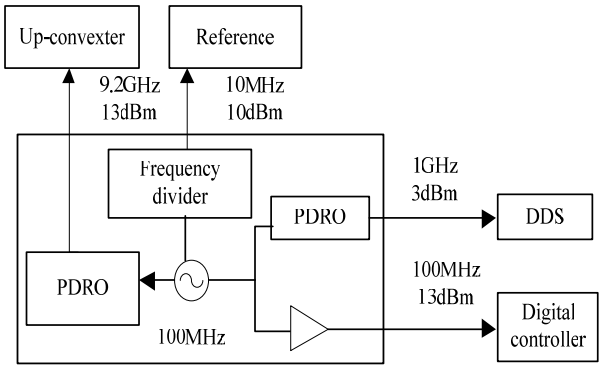

Figure 4. Diagram of the frequency synthesizer.

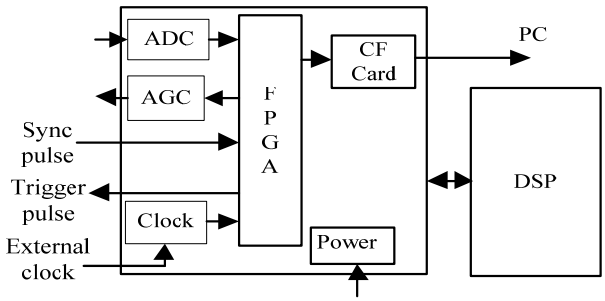

Figure 5. Diagram of the controller module.

to 10 MHz. Then, it passes through AGC, IF AMP to get adequate amplitude which can be offered to ADC for sampling and processing lastly.

Because the FMCW signal has large time-bandwidth product and needs low peak output power, the radar uses solid state power amplifier to meet the requirements of wide band and convenient use in application [14]. It consists of the following parts: preamplifier, power amplifier, power dividers, power synthesizers, power supplies, and control modules. To get the sum of the chirp signal and carrier signal, two mixers are used in the transceiver. One is used for frequency up-converting in transmitter and the other used for down-converting in receiver [15]. The radar uses a double balanced mixer, which has good isolation with the parasitic signal and local oscillator signal. At the same time, the mixer has high third order intermodulation to prevent saturation which may be caused by the leakage signal from the transmit module. Meanwhile, the filter is made up of cavity filter in the front for high frequency signal processing and LC filter in the end for intermediate frequency signal processing. Thus, the radio frequency filter is in the form of cavity filter, and the LPF, BPF are in the form of LC filter with lumped elements. The LPF before ADC in the receive module is used to eliminate the sum frequency of the received chirp signal and reference signal caused by the mixer [16].

Fourthly, frequency synthesizer is designed based on a stable local oscillator. The diagram of frequency synthesizer is shown in Fig. 4. It consists of a high temperature oscillator and phase-locked dielectric oscillator (PDRO), which provide stable reference signal for DDS module, up-converter and digital controller [17]. In addition, the frequency synthesizer provides reference signal for measure instruments such as spectrum analyzer and vector network analyzer. Thus, the frequency synthesis

is important for transmitter and receiver. The controller module's clock signal is generated by the frequency synthesis module too. Because the frequency synthesizer only provides reference signal of 9.2 GHz to the up-converter, and its frequency should be quadruplicated to arrive at the high frequency supplied to the mixer (36.8 GHz).

Finally, a controller module is developed based on field programmable gate array (FPGA) and DSP controller. Its diagram is shown in Fig. 5. The digital control centre is used for collecting data and storing data. In the meantime, it is also used for monitoring signal amplitude, changing the intermediate frequency amplifier to realize the ability of automatic gain control [18]. In the signal processing producer, FPGA is used to generate the radar's trigger signal in time and convert the target's echo signal to digital data with the data pre-distortion. Meanwhile, DSP is used to load the initial data and to calculate for the complex data processing procedure. To realize the task of data storing and processing, CF card is chosen as the storage media in the system [19]. In the meantime, a 16-bit ADC is implemented to digitalize the received signal for processing by the FPGA controller. To satisfy the system's requirement of rapid response and fast data storing speed, the ADC's sampling is 10 MHz, which is feasible based on the high internal operating frequency of the FPGA [20].

In a word, to acquire high range resolution for micro-deformation monitoring radar, we should carefully design the radar's system. In this article, parameters used in the radar are listed in Table 1.

Table 1. Radar parameters.

Parameters	Values
Central Frequency	36.05 GHz
Bandwidth	300 MHz
Transmitted Power	23 dBm
PRF	1 kHz
AD Sampling Rate	10 MHz
Sampling Precision	16 bit
Noise Figure	≤ 3.5 dB
Receiver's power consumption	≤ 2 W

4. EXPERIMENT OF RADAR PERFORMANCE VERIFICATION

4.1. Resolution Verification

Experiments are used to verify the accuracy and resolution of the radar. In the experiment, a corner reflector is installed on a guide rail, and the reflector is moved step-by-step. Each time, the corner reflector is moved by a distance of 1 mm. The guide rail's theoretical resolution ΔL is calculated by the following Equation (4).

$$\Delta L = \frac{L}{(360^\circ/\Delta\theta) \cdot N} \tag{4}$$

where L is the length of the rail's screw, $\Delta\theta$ the step angle of the guide rail's step motor, and N the subdivision number of the guide rail's step motor.

The experiment setup is shown in Fig. 6(a). As we know, the theoretical range resolution of the radar is smaller than 1 mm according to Equation (2). The experiment results are demonstrated in Fig. 6(b).

In the experiment, the corner reflector on the rail is placed in different positions at different times. The phase of the echo changes with the corner reflector's position. The parameters measured by the radar are given in Table 2. It is found that the averaged phase difference is 1.52 rad, and the standard deviation of the measured deformation is 56 µm. Based on Equation (2), we acquire that the averaged deformation of the corner reflector is 1.006 mm at each step. Therefore, the micro-deformation monitoring radar's resolution is smaller than millimetre. Meanwhile, the rail's theoretical precision is

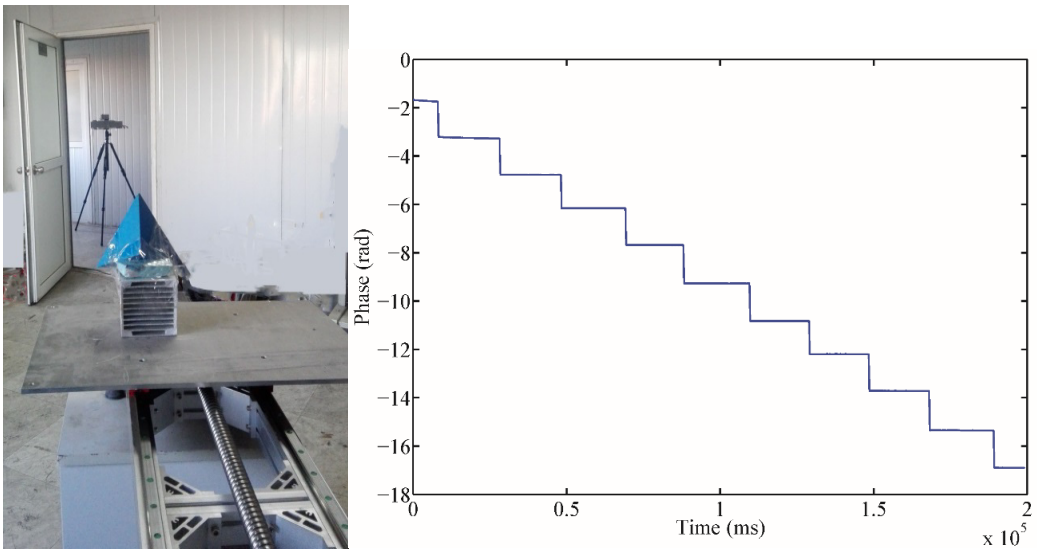

(a) (b)

Figure 6. Results of the railway guide experiment. (a) Experiment setup. (b) Results of phase measured by the radar.

Table 2. Echo's phase at different times.

Time Periods	8–28 s	28–48 s	48–68 s	68–88 s	88–108 s	108–128 s	128–148 s	148–168 s	168–188 s
Radians	−3.252	−4.776	−6.154	−7.683	−9.267	−10.82	−12.19	−13.72	−15.35

12.5 μm based on Equation (4). Thus, the radar can provide a super-precision too, which is equal to the standard deviation of the micro deformation measured by the radar (56 μm).

4.2. Accuracy Verification

Based on above analysis, the radar can measure micro deformation with a high precision and high resolution. If we use the radar in deformation monitoring regions, the radar should measure the deformation process timely and accurately. To verify the monitoring capabilities of the radar, an electrical shaking table is used in this experiment. The setup is shown in Fig. 7. Herein, the shaking table works on different frequencies and amplitudes at different times. The parameters used in the experiment are given in Table 3.

In this experiment, the radar is installed 6 meter far away from the shaking table. To get the spectrum of the vibration, fast Fourier transform (FFT) is used to analyse the experiment data shown in Fig. 8(a). The analysis result is shown in Fig. 8(b). It can be seen that the radar can measure the vibration's frequency accurately. Simultaneously, the vibration's amplitudes measured by the radar are equivalent to the pre-set values after the radar was calibrated. Thus, the radar can measure the vibration with high precision and accuracy.

Table 3. Parameters of the shaking table.

Time Periods	**Frequencies**	**Amplitudes**
10–40 s	19 Hz	1 mm
50–85 s	115 Hz	0.5 mm

Figure 7. Electrical shaking table.

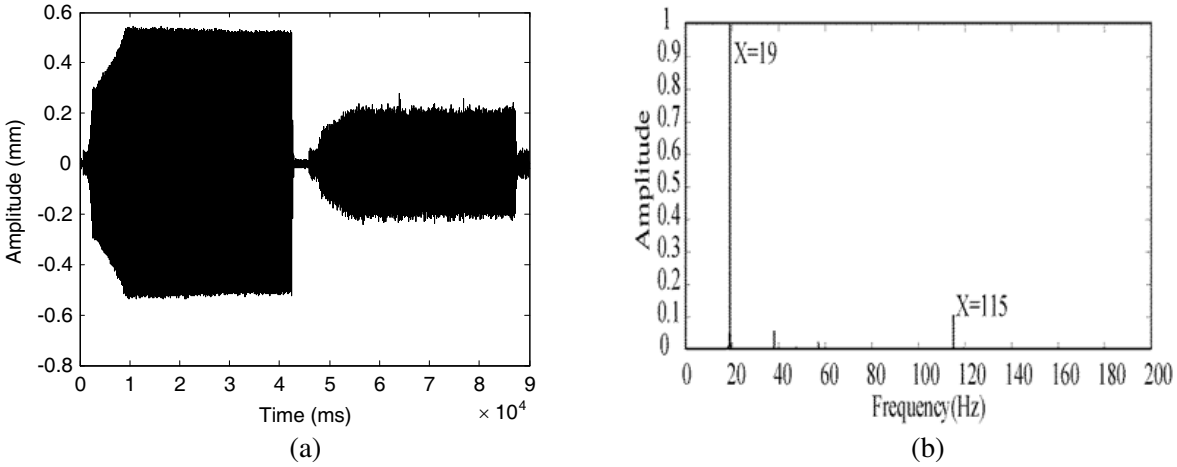

Figure 8. Experiment results of the shaking table. (a) Diagram of the shaking table's vibration. (b) Spectrum of the shaking table's vibration.

5. EXPERIMENT OF RAILWAY BRIDGE'S VIBRATION

To verify the effectiveness and accuracy of the radar, the micro deformation of a bridge on the Beijing Metro line 13 near north fourth Ring Road is measured. The light train of Line 13 has a length of approximately 116 m, which is composed of six 19-meter-long B-type carriages and five 0.4 m train connectors [21]. The speed of the subway is about 80 km/h. The radar is installed near the bridge, and it has an elevation angle of 20°. The radar is used to monitor the railway bridge's vibration when a train passes though the bridge. The experiment setup is shown in Fig. 9(a). The experiment result is shown in Fig. 9(b). From the experiment, it is found that the amplitude of the bridge's vibration is about 5 mm. The experiment result of the radar is consistent with that in [22]. Thus, the radar can be used to monitor a bridge's vibration. Meanwhile, the bridge vibration is obvious during the time between the tenth to the twentieth seconds, and the railway train passes through the bridge by using this time period. Because the length of the bridge is 84 m and the velocity of the train 80 km/h, the time used for passing through the bridge can be calculated by Equation (5).

$$t = L/v \tag{5}$$

where L is the sum of the length of the bridge and the length of the train. v is the velocity of the railway train.

It can also be seen that the obvious vibration of the bridge is mainly caused by the strike of the

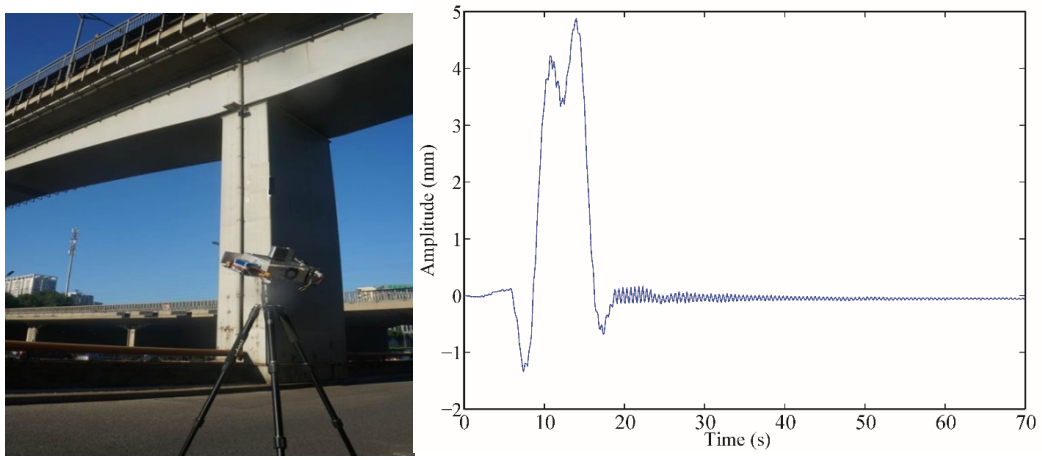

Figure 9. Experiment results of the railway bridge's vibration. (a) Experiment setup. (b) Vibration of the bridge.

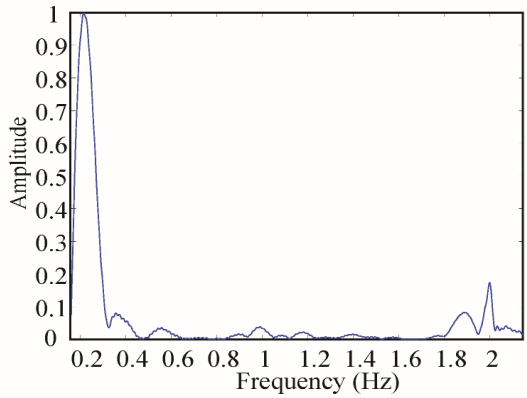

Figure 10. Spectrum of bridge vibrations in the entire time.

railway train as shown in Fig. 9(b). Certainly, the construction and material of the bridge can affect the bridge's vibration too. Thus, the bridge's vibration can be described by a system with multi-degree of freedom [23]. In order to analyse the vibration in detail, the spectrum of the vibration is obtained by using chirp Z-transform, and the result is shown in Fig. 10. To capture details of the bridge vibration's spectrum, we analyse the bridge vibration in two different time periods, namely 10–20 s and 60–70 s. The corresponding spectrums of the vibration in these two different time periods are shown in Fig. 11.

In Fig. 10, there are two peaks in the spectrum of the bridge vibration. One is the frequency of forced vibration located around 0.2 Hz, and the other is the natural frequency located around 2 Hz.

The frequency of forced vibration is dependent on the velocity of the light train and the length of the train. From the operation parameters of the Metro Line 13, the forced vibration frequency of the bridge can be calculated by Equation (6) [24]. It is 0.19 Hz, which is approximately equal to the forced frequency measured in Fig. 10.

$$f = v/l \tag{6}$$

In Fig. 11, it is obvious that the bridge vibration is composed of strong forced vibration which exists in the time during the tenth second to the twentieth second and weak free vibration which exists in the entire vibration time. From the experiment, it is concluded that the radar can acquire and distinguish the bridge's force vibration and free vibration [25]. Thus, the radar designed in the paper is effective and useful in micro-deformation monitoring field.

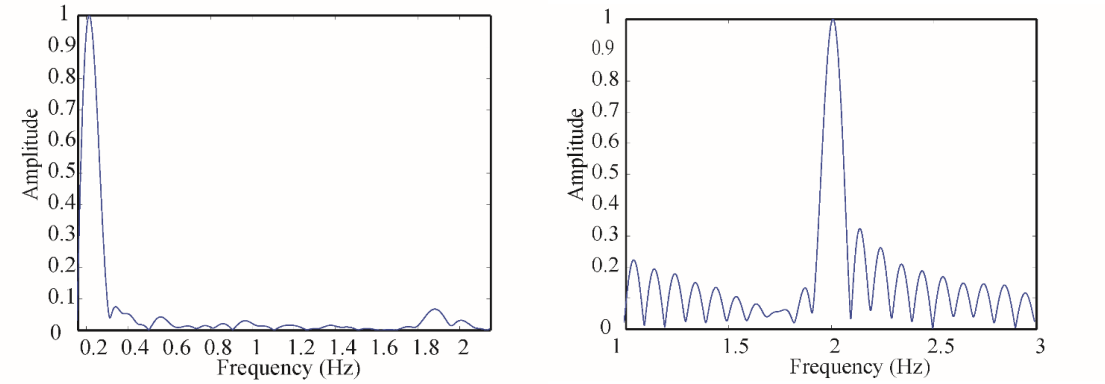

Figure 11. Spectrum of bridge vibrations in different time periods. (a) Spectrum of forced vibration. (b) Spectrum of free vibration.

6. CONCLUSION

Microradar has been proposed and designed using FMCW and differential interferometry techniques in this paper. The Ka-band radar can provide a super resolution and high precision in micro-deformation monitoring regions. In addition, the radar has been used in measuring vibrations of a bridge. The experiment results show that the radar has an accuracy of sub-millimetre, which makes the radar very suitable for micro-deformation monitoring regions. In the future, the radar will be used in monitoring the micro deformation of dams, slopes, high-rise buildings and others.

ACKNOWLEDGMENT

This work was supported by the National Key Research and Development Program of China (2016YFE0111100).

REFERENCES

1. Anonym, "Structural deformation surveying (EM 1110-2-1009)," US Army Corps of Engineers, Washington, DC, 2002.
2. Chen, Y. Q., "Analysis of deformation surveys — A generalized method," Technical Report of UNB's Department of Geodesy and Geomatics Engineering, 1983.
3. Ko, H. H., K. W. Cheng, H. J. Su, et al., "Range resolution improvement for FMCW radars," *Proceedings of the 5th European Radar Conference*, 352–355, Manchester, 2008.
4. Chang, M., C. P. Hu, P. Lam, et al., "High precision deformation measurement by digital phase shifting holographic interferometry," *Applied Optics*, Vol. 24, No. 22, 3780–3783, 1985.
5. Gentile, C., "Deflection measurement on vibrating stay cables by non-contact microwave interferometer," NDT&E International, Vol. 43, No. 3, 231–240, 2010.
6. Yiğit, E., A. Ünal, A. Kaya, et al., "Millimeter-wave round based synthetic aperture radar measurements," *URSI General Assembly and Scientific Symposium*, 13–20, Istanbul, F05-2, 2011.
7. Calvo-Gallego, J. and F. Pérez-Martínez, "Simple traffic surveillance system based on range-doppler radar images," *Progress In Electromagnetics Research*, Vol. 125, 343–364, 2012.
8. Hakobyan, A., P. M. Guire, D. Power, et al., "Applications and validation tests of ground-based coherent radar for deformation and vibration measurements in Canada's Atlantic region," *Proceeding of the IEEE 28th Canadian Conference on Electrical and Computer Engineering*, 638–642, Halifax, 2015.

9. Gentile, C. and G. Bernardini, "Radar-based measurement of deflections on bridges and large structures," *European Journal of Environmental and Civil Engineering*, Vol. 14, No. 4, 495–516, 2010.
10. Hyun, E. and J. Lee, "High precision range measurement processor design with low complexity for FMCW radar systems," *PIERS Proceedings*, 1662–1665, Prague, Jul. 6–9, 2015.
11. Liu, X. L., X. H. Tong, K. L. Ding, et al., "Measurement of long-term periodic and dynamic deflection of the long-span railway bridge using microwave interferometry," *IEEE Journal of Selected Topics in Applied Earth Observation and Remote Sensing*, Vol. 8, No. 9, 4531–4538, 2015.
12. Lu, X. D., F. M. Song, and J. J. Song, "Analyzing on phase error for single pass interferometric SAR," *The 3rd International Conference on Microwave and Millimeter Wave Technology Proceedings*, 489–492, Beijing, 2003.
13. Ayhan, S., V. V. Duy, P. Pahl, et al., "FPGA controlled DDS based frequency sweep generation of high linearity for FMCW radar systems," *The 7th German Microwave Conference*, Ilmenau, 2012.
14. Guo, Q. and S. G. Lv, "C-band solid state T/R module design for SAR application," *2009 Asia-Pacific Conference on Synthetic Aperture Radar*, 602–605, Xian, 2009.
15. Cheng, B. B., G. S. Jiang, C. Wang, et al., "Real-time imaging with a 140 GHz inverse synthetic aperture radar," *IEEE Transactions on Terahertz Science and Technology*, Vol. 3, No. 5, 594–605, 2013.
16. Abidin, Z. and A. Munir, "Development of FMCW SAR on L-band frequency for UAV payload," *The 10th International Conference on Telecommunication Systems Services and Applications*, Denpasar, 2016.
17. Bicici, C. and O. Cerezci, "Achieving frequency synchronization by GPS disciplined reference signal," *The 21st International Conference on Microwave, Radar and Wireless Communications (MIKON)*, Krakow, 2016.
18. Chua, M. Y. and V. C. Koo, "FPGA-based chirp generator for high resolution UAV SAR," *Progress In Electromagnetics Research*, Vol. 99, 71–88, 2009.
19. Chang, W., H. Tian, and C. Gu, "FMCW SAR: From design to realization," *IEEE International Conference on Geoscience and Remote Sensing*, 1122–1125, Beijing, 2016.
20. Hyun, E., Y. S. Jin, J. H. Lee, et al., "Design and implementation of 24 GHz multichannel FMCW surveillance radar with a software-reconfigurable baseband," *Journal of Sensors*, 1–11, 2017.
21. Zhang, Y., W. Zhai, X. Zhang, X. Shi, X. Gu, and Y. Deng, "Ground moving train imaging by Ku-band radar with two receiving channels," *Progress In Electromagnetics Research*, Vol. 130, 493–512, 2012.
22. Nakasuka, J., T. Mizutani, Y. Yamamoto, et al., "Analysis of large amplitude vibration mechanism of high-speed train PRC girder bridges based on vibration measurement," *The 6th International Conference on Advances in Experimental Structural Engineering*, Illinois, 2015.
23. Garinei, A. and G. Risitano, "Vibrations of railway bridges for high speed trains under moving loads varying in time," *Engineering Structures*, Vol. 30, No. 3, 724–732, 2008.
24. Li, J. Z. and M. B. Su, "The resonant vibration for a simply supported girder bridge under high speed trains," *Journal of Sound and Vibration*, Vol. 224, No. 5, 897–915, 1999.
25. Ju, S. H. and H. T. Lin, "Resonance characteristics of high-speed trains passing simply supported bridges," *Journal of Sound and Vibration*, Vol. 267, No. 5, 1127–1141, 2003.